

Electrochemical and Optical Properties of CeO₂-SnO₂ and CeO₂-SnO₂:X (X = Li, C, Si) Films

Marcos A.C. Berton, César O. Avellaneda*

Centro Multidisciplinar de Desenvolvimento de Materiais Cerâmicos, Laboratório Interdisciplinar de Eletroquímica e Cerâmica, Departamento de Química, Universidade Federal de São Carlos, C.P. 676, 13565-905 São Carlos - SP, Brazil

Received: November 22, 2000; Revised: October 21, 2001

Thin solid films of CeO₂-SnO₂ (17 mol% Sn) and CeO₂-SnO₂:X (X = Li, C and Si) were prepared by the sol-gel route, using an aqueous-based process. The addition of Li, C and Si to the precursor solution leads to films with different electrochemical performances. The films were deposited by the dip-coating technique on ITO coated glass (Donnelly Glass) at a speed of 10 cm/min and submitted to a final thermal treatment at 450 °C during 10 min in air.

The electrochemical and optical properties of the films were determined from the cyclic voltammetry and chronoamperometry measurements using 0.1 M LiOH as supporting electrolyte. The ion storage capacity of the films was investigated using *in situ* spectroelectrochemical method and during the insertion/extraction process the films remained transparent. The powders were characterized by thermal analysis (DSC/TGA) and X-ray diffraction.

Keywords: CeO₂-SnO₂ doped films, ion storage, sol-gel films

1. Introduction

There is a growing interest in the development of solid state electrochromic devices (ECD) such as smart windows, large area displays and rearview mirrors due to technological interest¹⁻³. Smart windows are characterized by their ability to vary the transmitted visible light as well as the solar radiation. In these systems when a small current flows through the electrochemical cell, the ions stored in the counter electrode diffuse towards the electrochromic layer and change its transmittance continuously over a wide spectral range and consequently alter the overall optical transmission of the device.

Despite of the importance of the counter-electrode for the operation of the ECD devices, their development has been slow compared to that of electrochromic films (*e.g.* WO₃) which have been extensively studied. The counter-electrode should offer high transmission in the visible range and small transmission change during the insertion/extraction of Li⁺ ions or protons and good kinetic properties. It must also have a sufficiently high charge capacity for the insertion of Li⁺ and protons.

A number of electrode materials has been proposed for this purpose like In₂O₃⁴, V₂O₅⁵, cerium oxide CeO₂⁶, as well as mixed oxides like CeO₂-TiO₂⁷⁻⁹, CeO₂-ZrO₂¹⁰⁻¹¹,

CeO₂-TiO₂-ZrO₂¹² and CeO₂-SnO₂^{13,14}. Baudry *et al.*⁶ have shown that CeO₂ coatings remain transparent during the lithium intercalation/deintercalation and that the reaction is reversible. Unfortunately, the reaction rate is too slow to be used in WO₃/CeO₂ cells. The first successful optically passive counter-electrode was based on CeO₂-TiO₂ and made by Baudry *et al.*⁶. The structure and the conductivity of CeO₂ films was modified by the substitution of titanium atoms for some atoms of Ce, using (NH₄)₂Ce(NO₃)₆ and alkoxide Ti(OPrⁱ)₄ as precursors.

This paper presents the optical and electrochemical response of CeO₂-SnO₂ counter-electrode with 17 mol% Sn and CeO₂-SnO₂ doped with Li, C and Si. These oxides, prepared by the sol-gel process show promising properties for the fabrication of electrochromic device. Sol-gel processing is a less expensive route to deposit such films over a large area compared to other methods and offers the advantage to control the film microstructure. This parameter influences the kinetics, durability and coloring efficiency.

2. Experimental

2.1. Preparation of the sol

The starting solution to produce CeO₂-SnO₂ (17 mol% of Sn) and CeO₂-SnO₂:X (X = Li, C and Si) was prepared

*e-mail: avelane@dq.ufscar.br

Trabalho apresentado no 14^o CBECIMAT, Águas de São Pedro, Dezembro de 2000.

using the route proposed by Orel *et al.*¹⁴ An aqueous solution was made dissolving 0.012 mol of $(\text{NH}_4)_2\text{Ce}(\text{NO}_3)_6$ and 0.002 mol of $\text{SnCl}_4 \cdot 5\text{H}_2\text{O}$ (17 mol% of Sn) as inorganic precursors. A precipitate was obtained by addition of NH_4OH at $\text{pH} = 9$. After washing the precipitate with bi-distilled water in order to remove the residual NH_4^+ , Cl^- , NO_3^- ions, the peptization was performed adding HNO_3 in equimolar quantity and water until the desired concentration. The colloidal sol was aged at a temperature up to 90°C for 20 min, giving a yellowish transparent sol. The final sol was then divided in four equal parts. The adding of dopants was performed as follow: in one part it was added 2 mol% of graphite powder, in another one it was added 15 mol% of LiNO_3 and in the third one it was added 50 mol% of GPTS [(3-Glycidylpropyl)trimethoxysilane].

2.2. Preparation of the films

The coatings for the spectroelectrochemical experiments were deposited on ITO coated glass by dip-coating with a pulling speed of 10 cm/min from a solution in ambient atmosphere ($\text{RH} \cong 60\%$). Previously, the ITO coated glass substrates (Donnelly Glass, $14\Omega/\square$) were cleaned and rinsed with bi-distilled water, ethanol and then dried at room temperature. The uniform gel films were then heat treated at 450°C for 10 min in air atmosphere. The process was repeated in order to obtain thicker films. A three layer coating had a thickness of about 100 nm. The films were transparent and homogeneous without any visual cracks. For electrochemical measurements, the geometrical area of the films was limited to 1.0 cm^2 by a Teflon tape.

2.3. Measurement techniques

Cyclic voltammetry and chronoamperometry experiments were performed with an EG&G PAR-263 computer-controlled potentiostat-galvanostat, driven by the M270 Electrochemical Analysis Software. A conventional three-electrode cell was used. The counter electrode was a platinum foil with an area of 1 cm^2 , and the pseudo reference electrode was a silver wire. The aqueous electrolyte was 0.1 M LiOH and the cell was previously purged with N_2 gas.

The optical transmittance and *in situ* UV-Vis spectroelectrochemical measurements of the films were performed on a model 5G Varian spectrophotometer, using a spectroelectrochemical cell with two flat glass windows.

Differential Scanning Calorimetry (DSC) and Thermal Gravimetry Analysis (TGA) were performed on powder samples with a Netzsch TASC414/2. All the analyses have been carried out in air atmosphere at a heating rate of $10^\circ\text{C}/\text{min}$.

X-ray diffraction measurements were performed on the powders obtained from the same sols after thermal treatment at 450°C for 10 min with a Siemens D5000 X-ray diffractometer with $\text{CuK}\alpha$ radiation.

3. Results and Discussion

The electrochemical response of the doped and undoped $\text{CeO}_2\text{-SnO}_2$ films was analyzed by cyclic voltammetry. This method determines the reversibility of the films to the intercalation and deintercalation of mobile ions. The 10th cyclic voltammogram for doped and undoped samples are depicted in Fig. 1, by sweeping the potential from -1.1 V to $+0.75\text{ V}$ at a scan rate of 50 mV/s . A cathodic and anodic waves are observed. The increase of the cathodic current at potential lower than -0.5 V is associated to the $\text{CeO}_2\text{-SnO}_2$ reduction with the simultaneous Li^+ insertion. On reversing the potential sweep direction, lithium deintercalation occurs. The oxidation process occurs close to -0.9 V and is followed by a peak at -0.55 V .

Figure 2 shows the cathodic and anodic charge densities of the $\text{CeO}_2\text{-SnO}_2$ and $\text{CeO}_2\text{-SnO}_2\text{:X}$ ($\text{X} = \text{Li}, \text{C}$ and Si) films obtained by chronoamperometry measurements during potential steps at intervals of 30 s from -1.1 V (insertion process) to $+0.6\text{ V}$ (deinsertion process) for the 10th cycle. No influence is observed in the intercalation process when C powder or lithium salt is added in the $\text{CeO}_2\text{-SnO}_2$ sol. On the other hand, when Si is added an increase occurs in the capacity of the intercalation process, which could be attributed to changes in the film structure.

The charge densities were $9.0\text{ mC}/\text{cm}^2$ ($\text{CeO}_2\text{-SnO}_2$), $7.7\text{ mC}/\text{cm}^2$ ($\text{CeO}_2\text{-SnO}_2\text{:Li}^+$), $7.7\text{ mC}/\text{cm}^2$ ($\text{CeO}_2\text{-SnO}_2\text{:C}$) and $10.6\text{ mC}/\text{cm}^2$ ($\text{CeO}_2\text{-SnO}_2\text{:Si}$). The last value is slightly higher from that obtained for pure CeO_2 oxide film¹³ ($8\text{ mC}/\text{cm}^2$) but similar to the results obtained for $\text{CeO}_2\text{-SnO}_2$ film¹⁴ and $\text{CeO}_2\text{-TiO}_2$ ⁶ film ($10\text{ mC}/\text{cm}^2$). However the charge densities are smaller than $\text{CeO}_2\text{-TiO}_2$

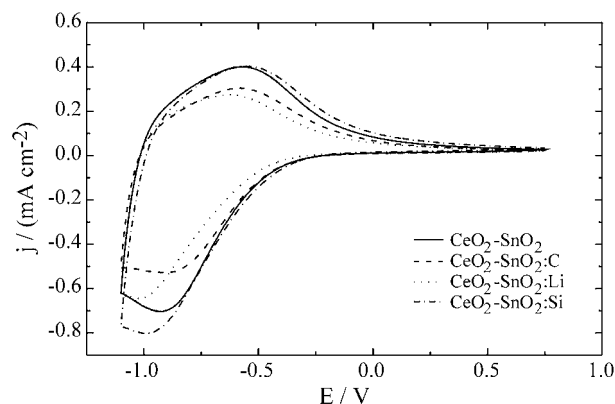


Figure 1. 10th cyclic voltammograms of $\text{CeO}_2\text{-SnO}_2$; $\text{CeO}_2\text{-SnO}_2\text{:Li}^+$; $\text{CeO}_2\text{-SnO}_2\text{:C}$ and $\text{CeO}_2\text{-SnO}_2\text{:Si}$ films measured at a potential scan rate of 50 mVs^{-1} in 0.1 M LiOH.

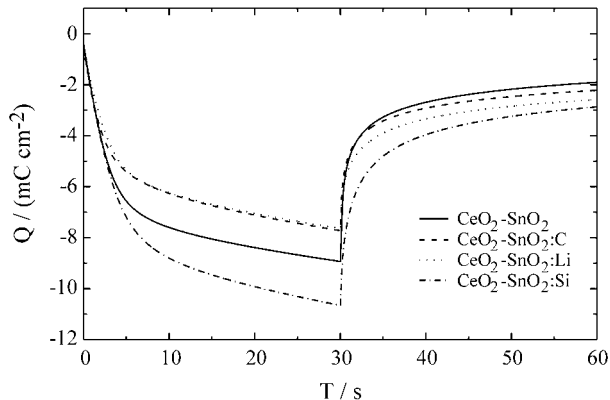


Figure 2. Cathodic and anodic transient charge densities for $\text{CeO}_2\text{-SnO}_2$; $\text{CeO}_2\text{-SnO}_2\text{:Li}^+$; $\text{CeO}_2\text{-SnO}_2\text{:C}$ and $\text{CeO}_2\text{-SnO}_2\text{:Si}$ films for the 10th cycle. Charged at $E = -1.1$ V, discharged at $E = +0.6$ V.

film (17 mC/cm^2)⁸ obtained with the same precursors as those made by Baudry *et al.*⁶ but using the sonocatalytic method.

The transmittance spectra for doped and undoped $\text{CeO}_2\text{-SnO}_2$ thin films were obtained by *in situ* measurements from 350 nm to 800 nm (Fig. 3). For all samples the films remained transparent during the intercalation/deinter-

calation process. The coloring/bleaching changes of the films depend slightly on the amount of the inserted/extracted charges. The lithiated film exhibits a higher transmittance at 550 nm giving 96% for intercalation and 97% for deintercalation (7.7 mC/cm^2), in comparison with $\text{CeO}_2\text{-SnO}_2\text{:Si}$ (10.6 mC/cm^2) giving 94% for intercalation and 95% for deintercalation processes.

The thermogravimetric analysis (TGA) and differential scanning calorimetry (DSC) for the $\text{CeO}_2\text{-SnO}_2$ powder are shown in Fig. 4. A large endothermic peak is observed in the DSC curve, and is accompanied by a weight loss of $\sim 3\%$ around 100°C that corresponds to the elimination of superficial water. This process continues up to $\sim 130^\circ\text{C}$ and is also accompanied by the exit of volatile products and/or elimination of residues. The total weight loss of this first process is about 6%. An exothermic peak ($\sim 320^\circ\text{C}$) is followed by an endothermic peak ($\sim 550^\circ\text{C}$), with a very accentuated weight loss $\sim 10\%$, probably associated with the dehydration of cerium hydroxide to cerium oxide and the oxidation of tin hydroxide to tin oxide. The formation of oxides are in agreement with the X-ray diffraction spectrum.

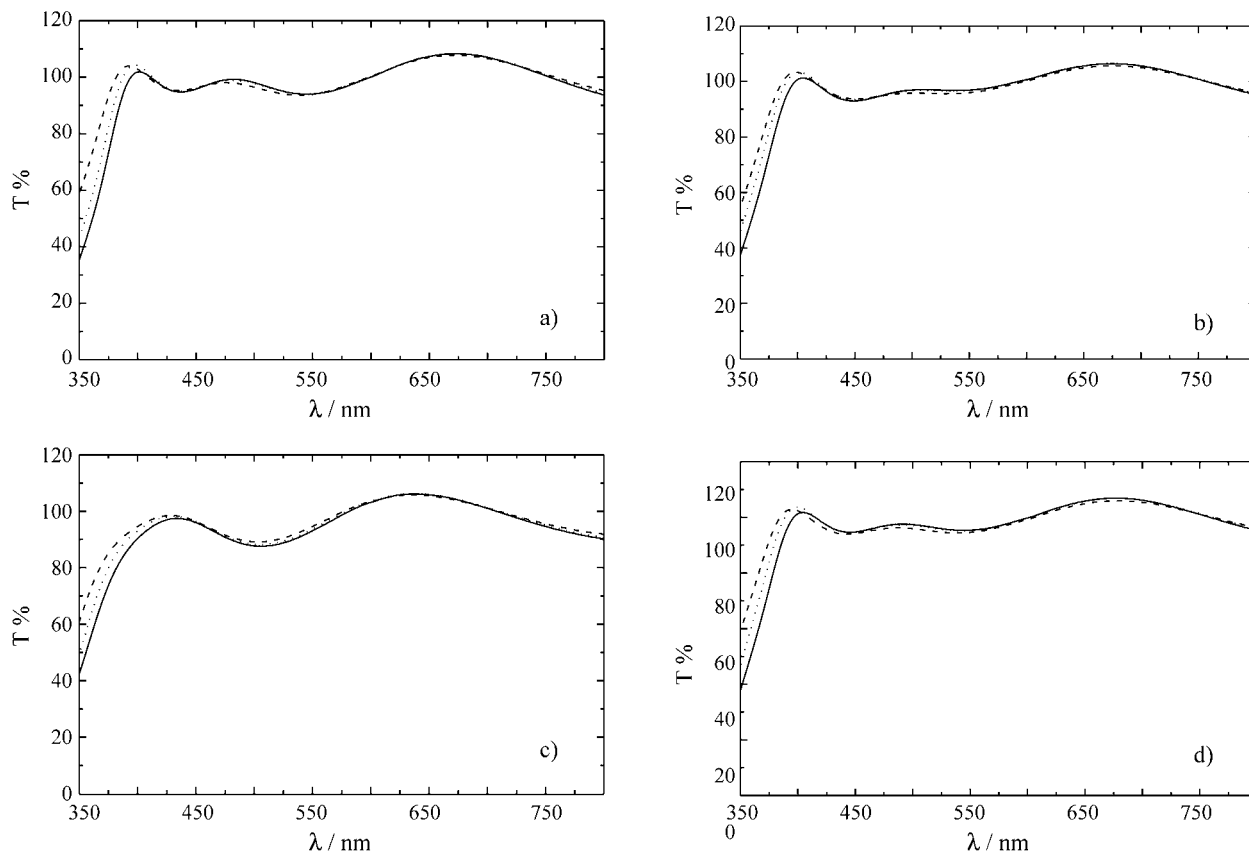


Figure 3. Transmittance (UV-VIS) spectra of: a) $\text{CeO}_2\text{-SnO}_2$; b) $\text{CeO}_2\text{-SnO}_2\text{:Li}^+$; c) $\text{CeO}_2\text{-SnO}_2\text{:C}$ and d) $\text{CeO}_2\text{-SnO}_2\text{:Si}$ films measured at the 10th cycle. (— as deposited); (--- $E = -1.1$ V) and (..... $E = +0.6$ V).

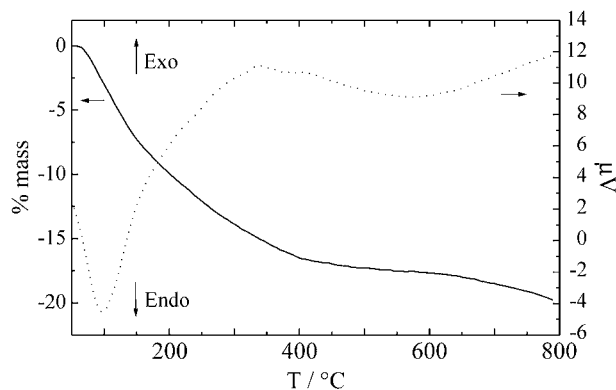


Figure 4. TG/DSC for $\text{CeO}_2\text{-SnO}_2$ powder, with 17 mol% of Sn.

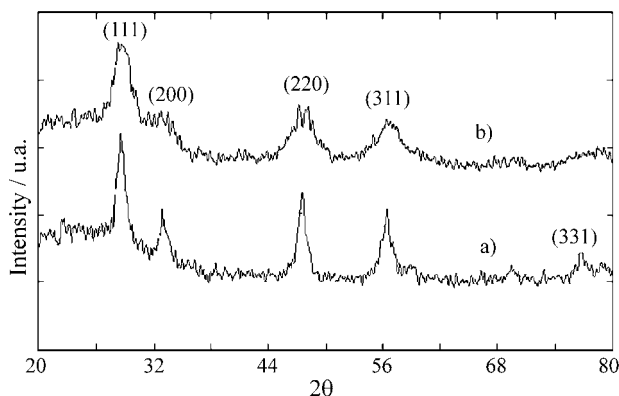


Figure 5. X-ray diffraction patterns of CeO_2 and $\text{CeO}_2\text{-SnO}_2$ powders heated at 450°C . (a) CeO_2 and (b) $\text{CeO}_2\text{-SnO}_2$.

The X-ray diffraction measurement of powders thermally treated at 450°C showed the formation of crystalline cerium oxide with peaks at $2\theta = 28.35, 33.13, 47.47, 56.33$ and 76.69 degrees (Fig. 5). According to the X-ray measurements, no shift in the peak position is observed with the SnO_2 addition, but only a small broadening of the diffraction lines was displayed. The broadening is related to the change in the film structure, suggesting that the doped film became less crystalline than the film without dopant. Similar results were reported by Orel¹⁴.

4. Conclusions

The sol-gel route via an aqueous-based process was successfully used for the preparation of thin solid films of $\text{CeO}_2\text{-SnO}_2$ (17 mol% Sn) and $\text{CeO}_2\text{-SnO}_2\text{:X}$ ($\text{X} = \text{Li}^+, \text{C}$ and Si). The films obtained exhibit promising electrochemical and optical properties. The highest charge density for the intercalation process was obtained for the Si doped

$\text{CeO}_2\text{-SnO}_2$ film (10.6 mC/cm^2). These results indicate that the changes in the doped film structure, when Si is added as dopant, are more pronounced. These properties confirm the possible use of these electrodes as an ion storage system for electrochromic smart windows.

Acknowledgment

The authors are grateful to FAPESP and CNPq for the financial support.

References

1. Granqvist, C.G. *Handbook of Inorganic Electrochromic Materials*, Elsevier, Amsterdam, 1995.
2. Aegerter, M.A. *Sol-Gel Chromogenic Materials and Devices in: Structure and Bonding*, 85, p. 149-194, Springer, Berlin Heidelberg, 1996.
3. Monk, P.M.S.K.; Mortimer, R.J.; Rosseinsky, D.R. *Electrochromism Fundamental and Applications*, VCH Weinheim, 1995
4. Cogan, S.T.; Anderson, E.J.; Plante, T.; Raugh, R.D. *Applied Optics*, v. 24, p. 2282, 1985.
5. Picardi, G.; Varsano, F.; Decker, F.; Opara-Krasovec, U.; Surca, A.; Orel, B. *Electrochimica Acta*, v. 44, p. 3157, 1999.
6. Baudry, P.; Rodrigues, A.C.M.; Aegerter, M.A.; Bulhões, L.O.S. *J. Non-Cryst. Solids*, v. 121, p. 319, 1990.
7. Keómany, D.; Petit, J-P.; Deroo, D. *Solar Energy Materials & Solar Cells*, v. 36, p. 397, 1995.
8. Avellaneda, C.O.; Pawlicka A. *Thin Solid Films*, v. 335, n. 1-2, p. 248, 1998.
9. Valla, B.; Tonazzi, J.C.L; Macedo, M.A.; Dall'Antonia, L.H.; Aegerter, M.A.; Gomes, M.A.B.; Bulhões, L.O.S *In Optical Materials Technology for Energy Efficiency and Solar Energy Conversion*, Proc SPIE., San Diego, CA, USA, v. 1536, p. 48, 1991.
10. Luo, X.; Zhu, B.; Xia, C.; Niklasson, G.A.; Granqvist, G.C. *Solar Energy and Solar Cells*, v. 53, p. 341, 1998.
11. Orel, Z.C.; Orel, B. *J. Mater. Sci.* v. 30, p. 2284, 1995.
12. Avellaneda, C.O.; Bulhões, L.O.S.; Pawlicka, A. *Proc. SPIE, Sol-Gel Optics V*, Dunn, Bruce S.; Pope, E.J.; Schmidt, H.K.; Yamane, M., eds., v. 3943, p. 306, 2000.
13. Stanger, U.L.; Orel, B.; Grabec, I.; Ogorevc, B; Kalcher., L. *Solar Energy Materials and Solar Cells*, v. 32, p. 171, 1993.
14. Orel, Z.C.; Orel B. *J. Mater. Sci.* v. 30, p. 2284, 1995.